

Structural and Optical Properties of Porous Silicon Prepared by Electrochemical Etching

Jeong Seok Lee and Nam Hee Cho[†]

Department of Materials Science and Engineering, Inha University, Incheon 402-751, Korea
(Received December 19, 2001; Accepted January 4, 2002)

ABSTRACT

The structural and optical features of Porous Silicon(PS) were investigated; the porous silicon was prepared by electrochemical etching of silicon wafers in HF solution. The morphologies and Photoluminescence(PL) features of the PS were investigated in terms of etching time, current density and aging conditions. The average pore diameter and pore depth were determined by current density and etching time, respectively. As-prepared PS exhibited the maximum PL peak at the wavelength of ~ 450 nm. The degree of deviation from as-prepared PS during aging treatment seemed to depend on the microstructure as well as morphology of the PS. It is found that etching current density played an important role on the microstructural features of the PS.

Key words : Porous silicon, Electrochemical etching, Photoluminescence, Aging, Current density

1. Introduction

In recent years, Porous Silicon(PS) has been widely studied mainly because of its optical properties which allow the realization of silicon based optoelectronics.^{1,2)} The observation of the Photoluminescence(PL) at room temperature with a few percent efficiency gave rise to a possibility that optical and electronic devices could be produced on a simple silicon chip.^{3,4)} A few research groups also reported that Electroluminescence(EL) could be obtained from the PS, even though the efficiency is very low.⁵⁾

Until now, there has been no theory unanimously accepted for the luminescence of the PS.⁶⁻⁹⁾ Among the several models proposed to explain the PL phenomena in the visible light, the quantum confinement model seems to be supported by many experimental and theoretical investigations.¹⁰⁻¹³⁾ But, serious contradictions exist between the predictions and a number of experimental results.

In order for such unique and useful phenomena of the PS to be applied in real electronic devices, a number of problems have to be solved.

- The efficiency of light generation should be increased.
- The intensity of the light emitted from relevant PL or EL devices should be kept constant with time.
- The devices made of the PS should have good mechanical strength and thermal stability.

The structural and PL features of the PS were investigated and samples were prepared by electrochemical etching. Some of the samples were subject to subsequent oxidation in air atmosphere to examine the variation of optical features of the PS with aging time.

2. Experimental Procedure

The etching system used in this experiment is shown schematically in Fig. 1. The PS was prepared by the electrochemical etching method of p-type (001) Si wafers of 4 Ω cm resistivity in HF solution. The electrolytes consisted of HF (49%):H₂O:C₂H₅OH=1:1:2 by volume. The electrolyte temperature was kept at 40°C; the distance between the anode and the cathode was 1.5 cm. The electrochemical etching was performed under a current density of 30 and 100 mA/cm² for various times.

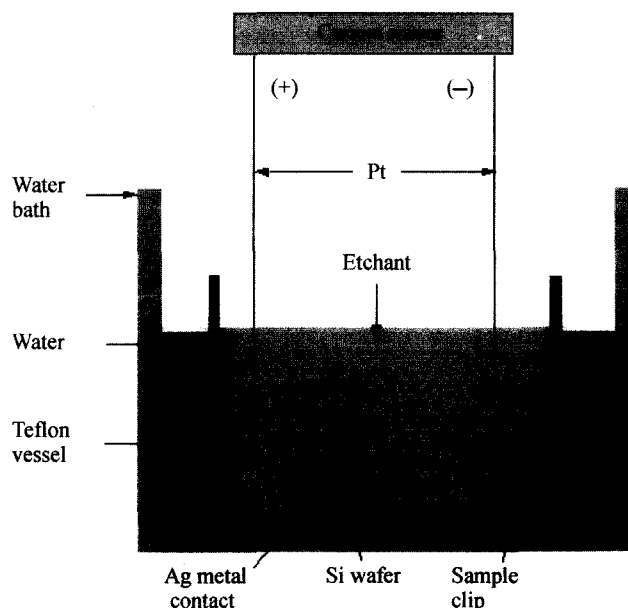


Fig. 1. Schematic diagram of the electrochemical etching system.

[†]Corresponding author : nhcho@inha.ac.kr

The surface and cross-section morphology was examined by a Scanning Electron Microscope (SEM, Hitachi, X-650). The PL was measured at room temperature by spectrofluorophotometer (Shimadzu, RF-5301). The chemical information was obtained by Fourier transform infrared spectroscopy (FT-IR, BIO-RAD, FTS-165) and the structural information was obtained by High-Resolution X-Ray Diffraction (HRXRD, Philip Xpert MRD).

3. Results and Discussion

A SEM flat-on image of the PS is shown in Fig. 2. The PS was anodized for 5 min at 30 mA/cm^2 in HF solution. The average pore diameter is approximately 9.2 nm, and the pores are distributed uniformly on the surface and separated with each other by about 9.5 nm.

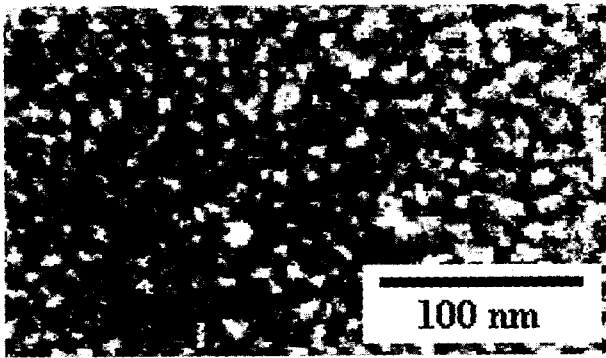


Fig. 2. Flat-on SEM images of the PS. The sample was etched at 30 mA/cm^2 for 5 min.

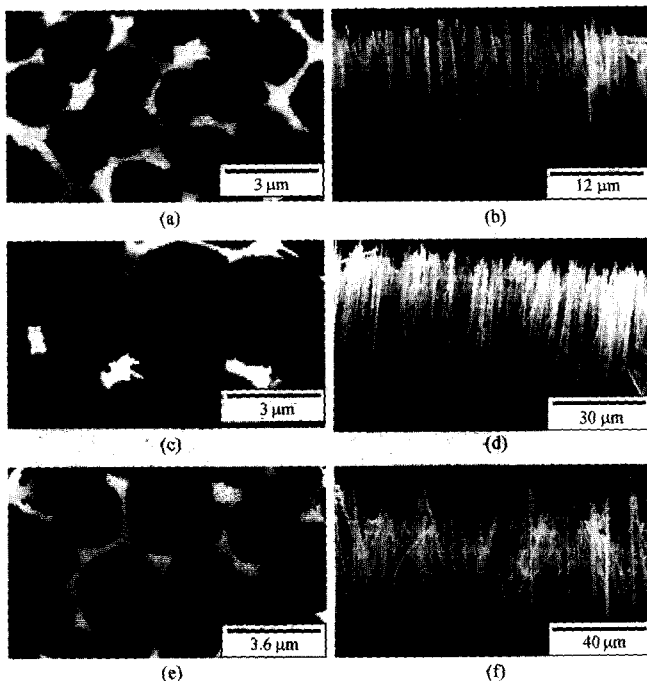


Fig. 3. SEM images of flat-on as well as cross-section views of the PS. These samples were etched at 100 mA/cm^2 for (a) and (b) 10 min; (c) and (d) 20 min; (e) and (f) 30 min.

Fig. 3 shows SEM images of flat-on as well as cross-section views of the PS. The PS was prepared at a current density of 100 mA/cm^2 for 10, 20 and 30 min. The flat-on view indicates that the pores are of a polygon-type column. The average diameter of the column-shaped pores in the PS is about

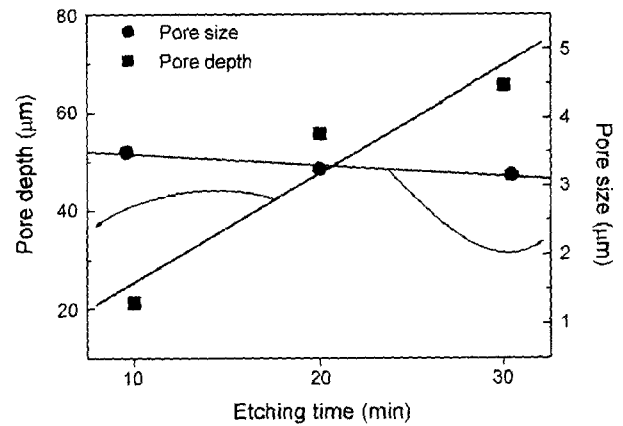


Fig. 4. Variation in the pore depth and pore size of the PS. These samples were etched at 100 mA/cm^2 .

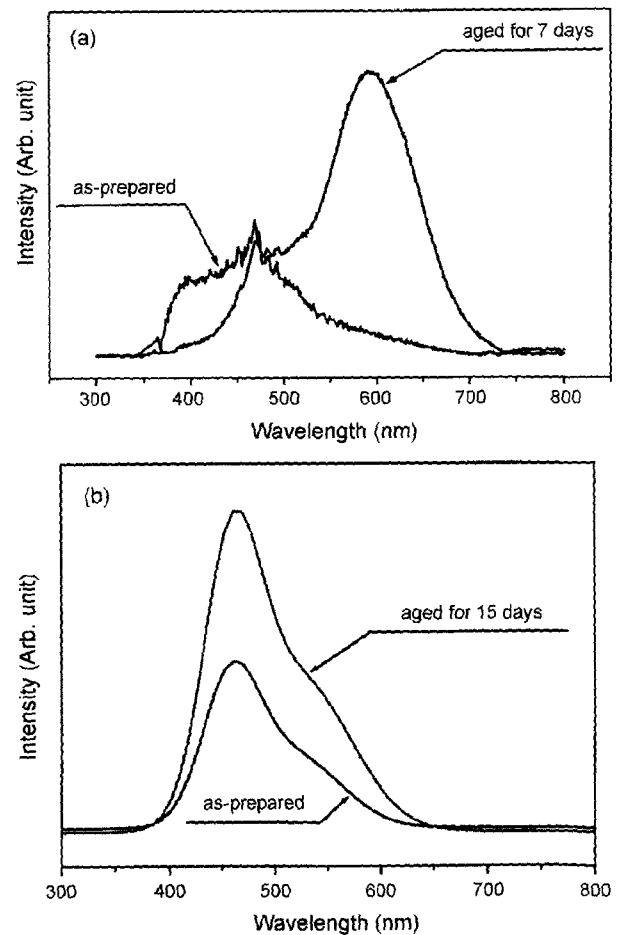


Fig. 5. Variation in the PL spectra of the PS with aging conditions and current densities. The PS was prepared by anodic etching at (a) 30 mA/cm^2 for 5 min; (b) 100 mA/cm^2 for 30 min.

3.3 μm , and these are separated by the walls of about 280-nm-thickness. In particular, the walls appear to have very uniform thickness, and stand perpendicular to the surface.

Fig. 4 shows that the pore depth increases with etching time. When the current density of 100 mA/cm^2 was applied, the etching rate was about $2.2 \mu\text{m/min}$. This indicates that the current density plays an important role on the distance between the pores, while the etching time determines the depth of the pore. The average diameter of the pore in the PS did not change with etching time. These results support the explanations of Beale model for the etching process of the p-type Si.¹⁴⁻¹⁷⁾

Fig. 5 shows the PL peaks of the PS prepared by aging the as-prepared PS in air atmosphere for particular time after etching silicon wafers at a current density of 30 or 100 mA/cm^2 . The as-prepared PS, prepared at current densities of 30 and 100 mA/cm^2 , exhibits the maximum PL peak at the wavelength of $\sim 450 \text{ nm}$. Both exhibit very similar PL spectral behaviors. From these results, we thought the observed PL

spectral features of the as-prepared PS etched at 100 mA/cm^2 might be caused by some structural characteristics of the 280-nm-thick walls rather than just by the thickness of the walls.

The intensities of red PL peaks of the PS, etched at 30 mA/cm^2 for 5 min, increase with aging time. When the as-prepared PS, prepared at 30 mA/cm^2 , is aged for 7 days in ambient air, the PL peak at a wavelength of $\sim 600 \text{ nm}$ increases significantly as shown in Fig. 5(a). However, the PS, prepared at 100 mA/cm^2 and aged for 15 days in ambient air, exhibits a prominent peak at a wavelength of $\sim 450 \text{ nm}$, and has only a shoulder peak at $\sim 550 \text{ nm}$. Aging in ambient air seems to affect the PL features of the PS in a different way, depending on the current densities at which the PS was prepared. Such a difference seems to be related with the microstructural and/or chemical features of the PS. To investigate the physical-chemical characteristics of the PS related with the observed PL variation with aging time, these samples were analyzed by FT-IR and HRXRD.

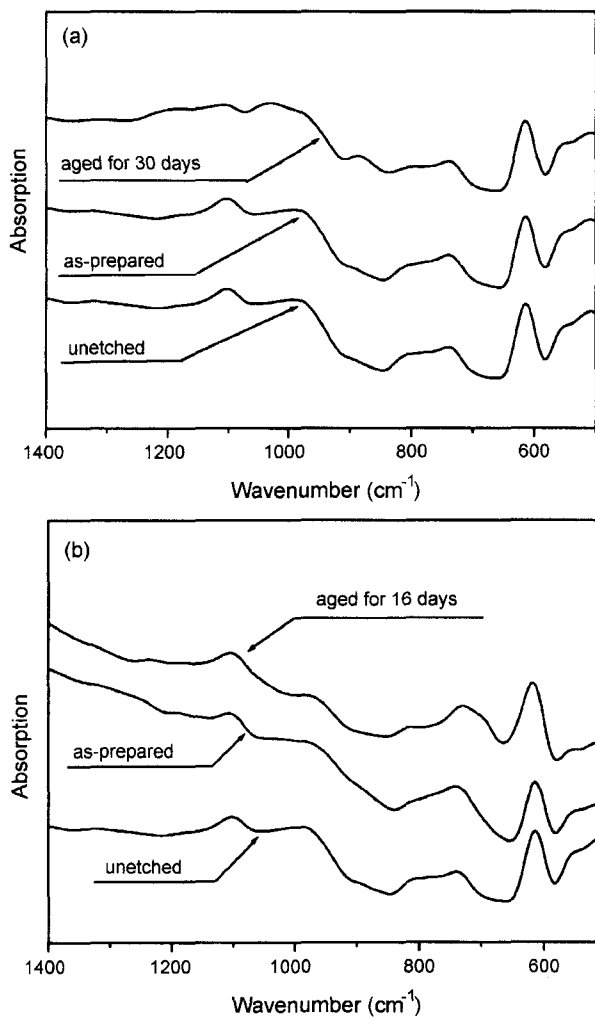


Fig. 6. Variation in the FT-IR spectra of the PS with aging conditions and current densities. The samples were prepared by anodic etching at (a) 30 mA/cm^2 for 5 min; (b) 100 mA/cm^2 for 30 min.

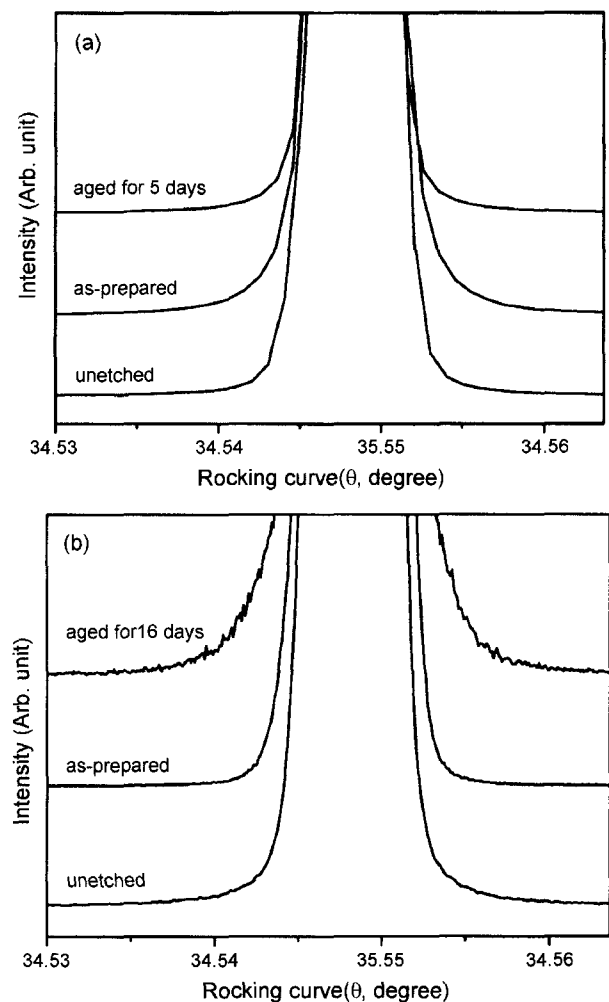


Fig. 7. Variation in the 004 peak of the HRXRD patterns of the PS with aging conditions and current densities. The samples were prepared by anodic etching at (a) 30 mA/cm^2 for 5 min; (b) 100 mA/cm^2 for 30 min.

The variation of the FT-IR spectra of the PS with aging treatment is shown in Fig. 6. It has been reported that the spectral features change significantly $1000 \sim 1200 \text{ cm}^{-1}$ in the spectra of post-etching thermal-treated PS; this is due to Si-O-Si vibration.^{18,19)} Although the as-prepared PS contains essentially no oxygen, it is expected that exposure to ambient air results in oxidation at the PS surface. The PS etched at 30 mA/cm^2 shows red PL, when the as-prepared sample was aged. But, the samples etched at 100 mA/cm^2 don't exhibit any prominent red PL, even after they were aged for 15 days. The FT-IR spectra of the aged PS seem to be different to each other in Fig. 6(a) and (b). The peaks at 900 and 1050 cm^{-1} seen in Fig. 6(a) seem to be related with the red PL; these are due to Si-O-Si bending.^{18,19)} From the comparison of the PL (in Fig. 5(a)) with the FT-IR results, the oxidation of the PS can be directly related with the observed red peak in the PL spectra.

The variation of HRXRD (004) reflection with the oxidation states of the PS is shown in Fig. 7. The samples were etched (a) at 30 mA/cm^2 for 5 min, and (b) at 100 mA/cm^2 for 30 min. The HRXRD results indicate that the intense and narrow Bragg peaks at $\theta = 34.55^\circ$ correspond to the diffraction peak of the silicon substrate, while some broad features were observed around the (004) peak of the diffraction curves in Fig. 7(b), after the as-prepared PS were aged for 16 days. On the other hand, the HRXRD patterns of the PS etched at 30 mA/cm^2 vary very little with aging treatment as shown in Fig. 7(b). From FT-IR and HRXRD results, the aging treatment produced oxidation and lattice distortion in the PS, but the degree or the amount of such deviation from as-prepared PS during aging treatment seem to depend on the microstructure as well as morphology of the PS.

4. Conclusion

The PS was prepared by electrochemical etching method and the pore distribution was uniform for all samples. The average pore diameter and pore depth were varied with current density, while the etching time plays an important role on the pore depth; in particular, when the current densities of 30 and 100 mA/cm^2 were applied, the pore diameters were $\sim 9.2 \text{ nm}$ and $3.3 \mu\text{m}$, respectively.

The as-prepared PS exhibits the maximum PL peak at a wavelength of $\sim 450 \text{ nm}$. But, when the as-prepared PS prepared at 30 mA/cm^2 is aged for several days in ambient air, the PL peak at a wavelength of $\sim 600 \text{ nm}$ increases significantly. The degree of deviation from as-prepared PS during aging treatment seems to depend on the structure as well as morphology of the PS. It is found in this study that etching current density plays an important role on such structural features of the PS.

Acknowledgement

This work was supported by Korea Research Foundation Grant (KRF-2001-005-E00009).

REFERENCES

1. S. M. Prokes, "Surface and Optical Properties of Porous Silicon," *J. Mater. Res.*, **11**(2), 305-320 (1996).
2. V. Parkhucic, "Porous Silicon-mechanisms of Growth and Applications," *Solid-State Electronics*, **43**, 1121-1141 (1999).
3. L. T. Canham, T. L. Cox, A. Loni and A. J. Simons, "Progress towards Silicon Optoelectronics Using Porous Silicon Technology," *Appl. Surf. Sci.*, **102**, 436-441 (1996).
4. J. P. Zheng, K. L. Jiao, W. P. Shen, W. A. Anderson and H. S. Kwak, "Highly Sensitive Photodetector Using Porous Silicon," *Appl. Phys. Lett.*, **61**(4), 459-461 (1992).
5. D. Dimova-malinovska, "Application of Stain-etched Porous Silicon in Light Emitting Diodes and Solar Cells," *J. Lumin.*, **80**, 207-211 (1999).
6. A. G. Cullis, L. T. Canham and P. D. J. Calcott, "The Structural and Luminescence Properties of Porous Silicon," *J. Appl. Phys.*, **82**(3), 909-965 (1997).
7. L. Tsybeskov, S. P. Dutttagupta, K. D. Hirschman and P. M. Fauchet, "Stable and Efficient Electroluminescence from a Porous Silicon-based Bipolar Device," *Appl. Phys. Lett.*, **68**(15), 2058-2060 (1996).
8. H. J. Cheon, D. J. Choi, S. K. Chang and E. D. Sim, "Deposition and Photoluminescence Characteristics of Silicon Carbide Thin Films on Porous Silicon," *J. Kor. Ceram. Soc.*, **35**(5), 486-492 (1998).
9. D. J. Choi, Y. J. Seo, H. J. Jeon, H. Y. Park and D. H. Lee, "Enhancement of Thermal Stability in Photoluminescence by Carbonization of Porous Silicon," *J. Kor. Ceram. Soc.*, **34**(5), 467-472 (1997).
10. Y. J. Seo, D. J. Choi, H. Y. Park and D. H. Lee, "Change in Photoluminescence of Porous Silicon with Processing Condition and Heat Treatment," *J. Kor. Ceram. Soc.*, **33**(10), 1170-1176 (1996).
11. C. Deleue, M. Lannoo, G. Allan and E. Martin, "Theoretical Descriptions of Porous Silicon," *Thin Solid Films*, **255**, 27-34 (1995).
12. O. Bisi, S. Ossicini and L. Pavesi, "Porous Silicon: A Quantum Sponge Structure for Silicon Based Optoelectronics," *Surface Science Reports*, **38**, 1-126 (2000).
13. I. M. Chang and Y. F. Chen, "Light Emitting Mechanism of Porous Silicon," *J. Appl. Phys.*, **82**(7), 3514-3518 (1997).
14. J. L. Gavartin, C. C. Matthai and I. Morrison, "The Influence of the Spatial Structure on the Electronic Properties of Porous Silicon: Quantum Chemical Study," *Thin Solid Films*, **255**, 39-42 (1995).
15. R. L. Smith and S. D. Collins, "Porous Silicon Formation Mechanisms," *J. Appl. Phys.*, **71**(8), R1-R22 (1992).
16. M. I. J. Beale, N. G. Chew, M. J. Uren, A. G. Cullis and J. D. Benjamin, "Microstructure and Formation Mechanism of Porous Silicon," *Appl. Phys. Lett.*, **46**(1), 86-88 (1985).
17. S. A. Campbell and H. J. Lewerenz, *Semiconductor Micromachining*, Vol. 1, pp. 299-302, Wiley, New York, 1998.
18. G. Socrates, *Infrared Characteristic Group Frequencies*, Vol. 1, pp. 126-128, Wiley, New York, 1980.
19. V. V. Filippov, V. P. Bondarenko and P. P. Pershukovich, "Excitation Spectroscopy of Anodically Oxidized Porous Silicon," *J. Lumin.*, **69**, 115-119 (1996).